Title

Bioelectricity generation by wetland plant-sediment microbial fuel cells (P-SMFC) and effects on the transformation and mobility of arsenic and heavy metals in sediment.

Journal

Environmental geochemistry and health, 41(5)

ISSN

0269-4042

Authors

Zhu, Juanping
Zhang, Taiping
Zhu, Nengwu
et al.

Publication Date

2019-10-01

DOI

10.1007/s10653-019-00266-x

Peer reviewed

Environ Geochem Health (2019) 41:2157–2168
https://doi.org/10.1007/s10653-019-00266-x

ORIGINAL PAPER

Bioelectricity generation by wetland plant-sediment microbial fuel cells (P-SMFC) and effects on the transformation and mobility of arsenic and heavy metals in sediment

Juanping Zhu · Taiping Zhang · Nengwu Zhu · Chunhua Feng · Shaoqi Zhou · Randy A. Dahlgren

Received: 29 January 2018 / Accepted: 21 February 2019 / Published online: 9 March 2019

Abstract Two wetland plant-sediment microbial fuel cell systems (PSM1 and PSM2) and one wetland sediment microbial fuel cell system (SM) were constructed to investigate their electricity production performance and the simultaneous migration and transformation of arsenic and heavy metals in sediment and overlying water, arsenic and heavy metals uptake by plants. The bioelectricity generation was monitored for 175 days, and sediment samples were collected at three time points (64, 125 and 200 days) for the analysis. The results showed that plants improved the efficiency of the electricity production by the fuel cell system. The average output voltage was: PSM1 (0.32 V) > PSM2 (0.28 V) > SM (0.24 V)($P \leq 0.05$).The electricity production of the electrodes and the introduction of plants affected the mobility and transformation of As, Zn and Cd in the sediment, which contributed to their stability in the sediment and reduced the release of these metals into the overlying water column. The bioelectricity production process affected the bioavailability of arsenic and heavy metals in the sediment and attenuated metal uptake by plants, which indicated the potential for remediation of arsenic and heavy metals pollution in sediment.

Keywords Wetland plant-sediment microbial fuel cell · Bioelectricity generation · Arsenic and heavy metals · Bioavailability

J. Zhu · T. Zhang (✉) · N. Zhu · C. Feng · S. Zhou (✉)
College of Environment and Energy, South China University of Technology,
Guangzhou 510006, Guangdong, People's Republic of China
e-mail: lckzhang@scut.edu.cn

S. Zhou
e-mail: fesqzhou@scut.edu.cn

T. Zhang · N. Zhu · C. Feng
The Key Lab of Pollution Control and Ecosystem Restoration in Industry Clusters, Ministry of Education, South China University of Technology,
Guangzhou 510006, Guangdong, People's Republic of China

S. Zhou
Guizhou Academy of Sciences,
Guiyang 550001, Guizhou, People's Republic of China

R. A. Dahlgren
Department of Land, Air and Water Resources, University of California, Davis, CA 95616, USA

Introduction

Most global urban river sediments are severely polluted with nutrients including nitrogen and phosphorus (Stortelder 1995; Duan et al. 2016; Noe et al. 2016), heavy metals (Audry et al. 2004; Deng and Dong 2016), and refractory organics, such as polycyclic aromatic hydrocarbon (PAH), polychlorinated biphenyls (PCBs) (Sarria-Villa et al. 2016; Hung et al.

2015). Heavy metals are the most prevalent pollutants and are generally the most common and severe in urban river sediments (Zhang et al. 2012; Islam et al. 2015). Kadhum et al. (2015) evaluated the metal concentrations in the surface sediments of the Langat River and found high levels for four heavy metals: Sn, 114 mg/kg; Cr, 21 mg/kg; Ni, 7.8 mg/kg; Cd, 0.59 mg/kg. In the past decade, the concentrations of Pb, Zn, Cd, Cu and Cr have increased in sediments from Swan Lake and Rongcheng Bay in the northern Yellow Sea due to fluvial transport, direct domestic discharge, industrial effluents and atmospheric deposition (Huang et al. 2013). Methods for remediating heavy metals in sediments include physical, chemical and biological technologies (Nejad et al. 2018). Physical and chemical methods, such as adsorption, ion exchange and electrochemical treatment, may be ineffective and/or very expensive. In contrast, biological methods are widely employed because of the wide range of available organisms for remediation and their generally high efficiency for the removal of heavy metals from sediment (Volesky and Holan 1995).

Microbial fuel cells (MFCs) are a novel technology to produce electricity. The working principle is to allow electrogenesis microorganisms to concentrate on the anode surface, and under anaerobic conditions, the microorganisms catalytically oxidize organic compounds to produce electrons and protons. The electrons are passed via an external circuit to the cathode, and the protons are passed through a proton exchange membrane to the cathode. MFC electricity production involves five steps: substrate biological oxidation, anode reduction, electronic transmission through an external circuit, proton transfer and cathode reaction. MFCs are widely used and have the potential to simultaneously remediate contaminated sediment, wastewater and waste leachate while generating electricity. Some researchers have examined heavy-metal treatment of wastewater using MFCs (Wang et al. 2008; Tandukar et al. 2009; Lefebvre et al. 2013).

Heijne et al. (2010) used MFCs to recycle copper-containing waste streams. They obtained copper removal rates as high as 99.88% and formed pure copper crystals on the cathode electrode. To investigate the removal efficiency of zinc and cadmium in wastewater, Abourached and coworkers established a single-chamber microbial fuel cell and demonstrated removal efficiencies of 90% and 97% for zinc and cadmium from wastewater, respectively, and a power density reaching 3.6 W/m^2 (Abourached et al. 2014). However, there is a paucity of research investigating microbial fuel cells to remediate heavy metals in contaminated soil and sediment. Wang et al. (2016) constructed a soil MFC to remediate the contaminated soil, and the electric field was generated from the oxidation of the acetate at the anode. They obtained the maximal voltage and power density of 539 mV and 65.77 m W/m(2) in the soil MFC, and the soluble Cu form and the total Cu contents from the anode to the cathode increased, and the difference between them kept growing over time. The electricity production process of microbial fuel cells may affect the form and valence state of heavy metals in sediment. Altering the redox status affects the migration behavior of heavy metals in sediments, so it is critical to study the redox changes and effects on heavy metals of microbial fuel cells during electricity production.

The purpose of this study is to innovate the wetland plant-sediment microbial fuel cells (P-SMFC) and probe the bioelectricity generation by P-SMFC and the effects on the transformation and mobility of heavy metals in sediment in the bioelectricity production process, so as to explore the potential for remediation of heavy-metal pollution in sediment. In this study, plant-sediment microbial fuel cells were constructed and applied to remediate river sediments polluted by heavy metals. The prevalent metalloid arsenic and heavy metals (Cd and Zn) in the Pearl River Delta sediment were selected to investigate their migration and transformation in sediments within plant-sediment microbial fuel cells (P-SMFCs). These heavy metals were selected due to their different toxicity levels, redox potentials, and chemical interactions with sediments. Arsenic and cadmium are the most toxic metalloid/heavy metal, while zinc is considerably less toxic. Meanwhile, the electricity performance of contrasting fuel cell systems (with and without plants) was evaluated over a 175 day period.

Materials and methods

Experimental layout

The three experimental devices were tested, as shown in Fig. 1, including a plant-sediment system (PS), sediment microbial fuel cell (SMFC) and wetland

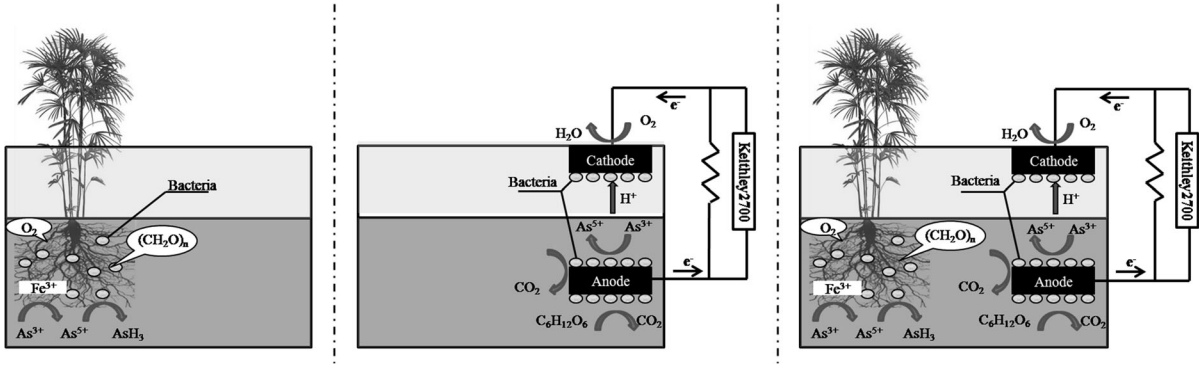

Fig. 1 Schematic diagrams of the three types of devices and their basic processes

plant-sediment microbial fuel cell (P-SMFC). Each of them was constructed using a polymethyl methacrylate (acrylic) cylinder (40 cm inner diameter, 40 cm height) with a sediment depth of 15 cm and overlying water (50 mM NaCl solution) depth of 5 cm. Sediments were collected from Guangzhou Chebei River (a branch of the Pearl River in the Guangzhou urban area) and mixed with mine-tailing soil (collected from the Qingxin gold mining area) in a 100:1 proportion. The physical and chemical properties of the mixed sediment are shown in Table 1. Two pieces of square, activated carbon fiber felt (100 cm^2 projected surface area) were used as the anode, which was placed 7–8 cm in the sediment from the bottom of the reactor. The activated carbon fiber felt was pretreated with acetone and nitric acid (Zhu et al. 2011). A graphite disk (10 cm diameter and 1 cm thickness) was used as the cathode, which was suspended on the overlying water surface with nylon mesh.

Cyperus alternifolius and short leaf *Cyperus malaccensis* were planted in the sediment 10 cm from the anode to form the P-SMFCs. The two electrodes were connected to a 1000 Ω external resistance using copper wire. The experimental design consisted of five treatments: two plant-sediment microbial fuel cell treatments (*C. alternifolius* + electrode treatment PSM1 and a short leaf *C. malaccensis* + electrode treatment PSM2); one sediment microbial fuel cell treatment (SM); and two treatments with plants but without connected electrode, one was *C. alternifolius* with no electrode (PS1) and the other was short leaf *C. malaccensis* with no electrode (PS2). Each of the five treatments was conducted in triplicate. All experiments were carried out outdoors under ambient conditions with no supplemental addition of nutrients.

Analytical methods

The voltage across the resistance (R = 1000 Ω) was measured and recorded every 180 s over 175 days using a data acquisition system (Model 2700, Keithley Inc., Solon, OH, USA). The current density (I, mA/m^2) and power density (P, mW/m^2) were normalized to the anode projected area (S = 0.01 m^2) and calculated as I = U/RS and P = IU, where U is the voltage (V) and R is the resistance. The polarization curves and power density curves were obtained by varying the external resistance from 90,000 to 50 Ω, as described by Logan et al. (2006). The system internal resistance was estimated from the slope of the linear segment of the polarization curves.

After 64, 125 and 200 days of operation, sediment samples (0–10, 10–20 and 20–30 cm from the anode) and the overlying water were collected. The water samples were filtered through a 0.45-μm microporous membrane filter prior to metal quantification. The

Table 1 Physical and chemical properties of the initial sediment

	Moisture content (%)	Organic matter (g/kg)	NH_4^+ (mg/kg)	NO_3^- (mg/kg)	TP (g/kg)	As (mg/kg)	Zn (mg/kg)	Cd (mg/kg)
Sediment	59.6	27.9	85	57	1.5	234	156	1.4

sediment samples were air-dried at room temperature, ground in an agate mortar and sieved through a 149-μm sieve. The total Cd and Zn concentrations were determined by HNO_3–HF–$HClO_4$ digestion in sealed Teflon vessels (Dalman et al. 2006). The concentrations of Cd and Zn were determined by graphite-furnace atomic absorption spectrophotometry and flame atomic absorption spectrometry (Z-200, Hitachi Limited, Japan), respectively. The detection limits for Cd and Zn were 0.01 and 0.005 μg/L, respectively.

The total arsenic concentration in the sediment samples was determined using an aqua regia digestion (Das et al. 2004). Solid-phase As was further fractionated into four operationally defined fractions using the BCR sequential extraction method (Baig et al. 2009). In brief, the sequential extraction method was the following: (1) acid-soluble fraction: 1 g of sample in 40 mL of 0.11 M CH_3COOH, shaking time of 16 h and centrifugation; (2) reducible fraction: 40 mL of 0.5 M NH_2OH–HCI (pH = 1.5), shaking time of 16 h and centrifugation; (3) oxidizable fraction: 10 mL of 30% H_2O_2, heating at 85 °C for 1 h (twice); then, addition of 40 mL of 1 M CH_3COONH_4 (pH = 2), shaking time of 16 h and centrifugation; (4) residual fraction: 4 mL aqua regia (HCI/HNO_3, 3:1) and heating at 85 °C for 1 h. The arsenic concentrations were measured by atomic fluorescence spectrometry (AFS-9130, Titan Instruments, Beijing) with a detection limit of 0.5 μg/L.

In the measurement process, in order to ensure the quality of monitoring, the reagents selected in the experiment were all pure reagents. Meanwhile, the blank tests were carried out to eliminate the error caused by the introduction of the reagent. Moreover, according to Technical Specifications for Soil Environmental Monitoring (HJ-T 166-2004, China) and Technical Guidelines for Environmental Monitoring and Analysis Methods Standard Revision (HJ-T 168-2010, China), in each batch of samples, parallel double-samples were taken for quality control. The indoor relative standard deviation of parallel double-samples met the precision and eligibility range, with 30% for cadmium, 20% for zinc and 20% for arsenic. In addition, the test value of the quality control samples was within the guaranteed value of the quality control sample (95% confidence level).

Before the system was running and after 200 days of operation, plant (above-ground) samples were collected and rinsed 2 ~ 3 times with deionized water. The plant samples were heated at 105 °C for 30 min, dried at 60 °C for 24 h, mulled and sieved through a 2-mm nylon mesh and reserved in a glass bottle. The As, Cd and Zn concentrations in the plants were determined by HNO_3–$HClO_4$ digestion in a conical flask (Simmons et al. 2005; Yin et al. 2016).

Statistical analysis

Excel 2007 (Microsoft Inc., USA) was used for recording and analyzing the raw data; Origin 8.5 (OriginLab, USA) was used to prepare the graphics. SPSS (ver.19.0) (IBM Inc., USA) was used for all the statistical analyses; all statistical analyses were evaluated at a $P \leq 0.05$ level of significance.

Results and discussion

Electricity production performance of P-SMFC

The voltage profiles for the P-SMFC and SMFC treatments over the 175-day measurement period are shown in Fig. 2. At the system startup, the open-circuit voltages of the PSM1, SM and PSM2 treatments immediately were 0.37, 0.30 and 0.41 V, respectively. During the 175 days of operation, the three treatments maintained a relatively stable electricity production in the output voltage range of 0.20–0.50 V. Within 75 days of the system initiation, the PSM1, SM and PSM2 treatments acquired a stable output voltage followed by a considerable fluctuation with the increasing time. This phenomenon may be explained by the loss of microbially labile organic matter surrounding the electrode due to microbial consumption. The transfer of organic matter from the sediment to the electrode may be variable over time, leading to variations in the output voltage. Over the entire experimental period, the maximum output voltages of the PSM1, SM and PSM2 treatments were 0.69, 0.66 and 0.63 V, respectively. The average output voltage was PSM1 (0.32 V) > PSM2 (0.28 V) > SM (0.24 V) at $P \leq 0.05$, which demonstrates that plants in the system increased the electricity production performance of the MFC relative to the system without plants. Plant root exudates may provide an important source of microbially labile carbon, leading to the

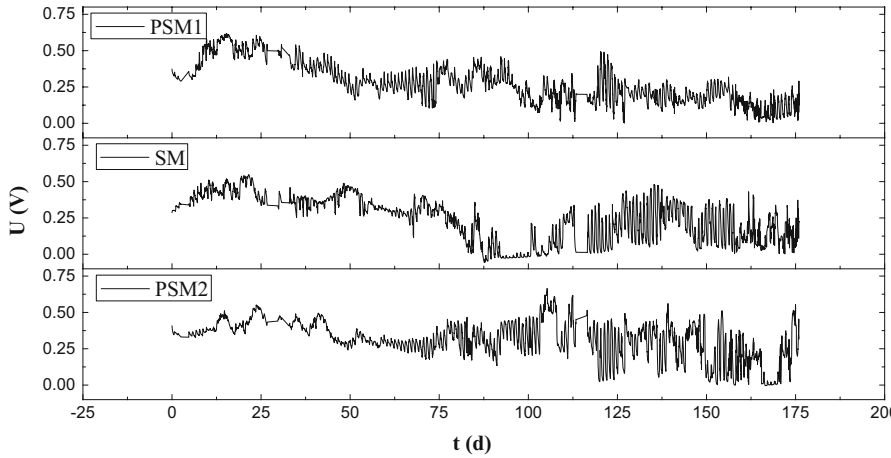

Fig. 2 Real-time voltage curves

increase in electrical production in the P-SMFC treatments.

The performance of the PSM1, SM and PSM2 treatments is depicted by the power density curves and polarization curves (Fig. 3). The plant treatments (PSM1 and PSM2 treatments) effectively enhanced the electricity generation. The open-circuit voltages of PSM1 and PSM2 were 0.721 and 0.716 V, respectively, and the maximum power densities of PSM1 and PSM2 were 10.74 and 10.05 mW m^{-2}, respectively, which were far greater than those for the SM treatment (0.661 V and 7.90 mW m^{-2}). Previous research has demonstrated that plants increased the output power density to seven times higher than that of sediment microbial fuel cells without plants (Dalman et al. 2006). Further, there was no effect on the plant growth, which effectively addressed the traditional sediment microbial fuel cell loss of organic matter transfer over time (Schamphelaire et al. 2008). The internal resistances of PSM1, SM and PSM2 were 602, 498 and 636 Ω, respectively (Fig. 3). The internal resistances for the PSM1 and PSM2 treatments were significantly ($P \leq 0.05$) higher than that of the SM treatment, which indicated that plants can increase the internal resistance of the system.

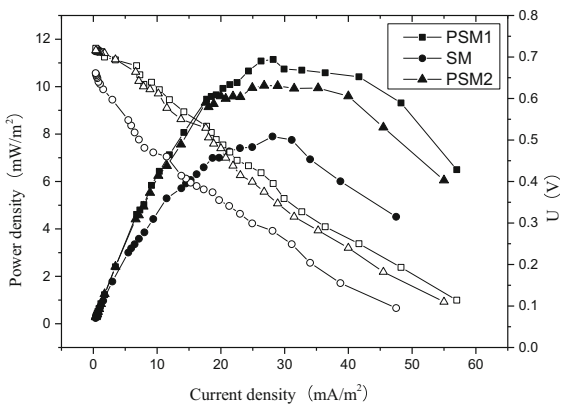

Fig. 3 Polarization and power density curves for the different treatments. The solid represents polarization, and the hollow represents power density

Influence of the P-SMFC electricity production on arsenic dynamics in sediments

The concentrations of total arsenic at each sampling point (distance from anode = 0–10 cm, 10–20 cm and 20–30 cm) for each treatment and sampling time are reported in Fig. 4. The arsenic concentrations for all the treatments significantly decreased at each sampling point with the increasing time. Moreover, the PS1 and PS2 treatments decreased faster than the PSM1, SM and PSM2 treatments. After 64 days (T0 time point), the total As concentrations were not significantly different among the treatments. In contrast, at 125 and 200 days (T1 and T2 time points), the total As concentrations of the PS1 and PS2 treatments were significantly lower than that of the PSM1, SM and PSM2 treatments, but there was no significant difference between the PSM1, SM and PSM2 electrode treatments (Fig. 4a). With increasing time, the total As concentrations for all treatments were significantly lower at the 10–20 cm distance from the anode than at the 0–10 cm distance; there was no significant difference among treatments (Fig. 4b). The treatments with plants had higher As concentrations at 20–30 cm

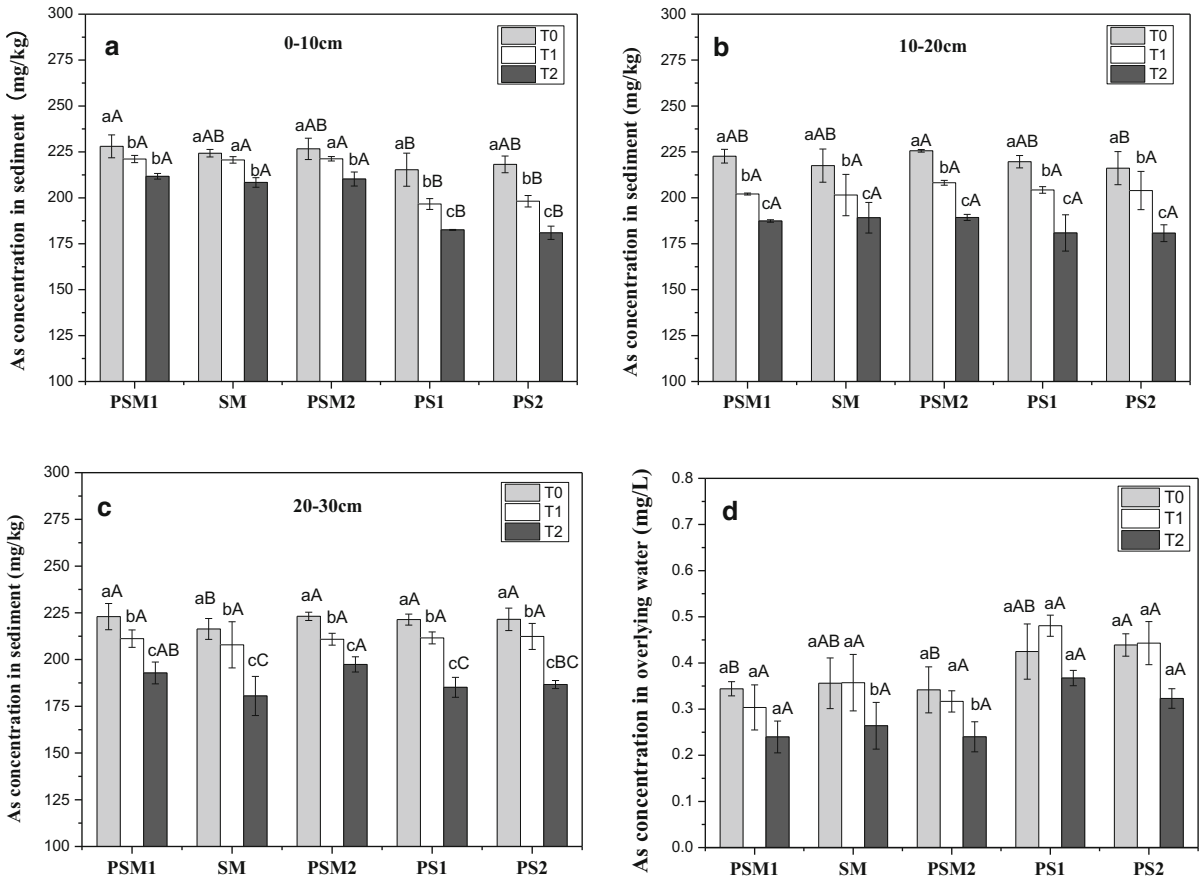

Fig. 4 Concentrations of total arsenic in the sediment and overlying water column (average of three replicates ± standard deviation). Lower-case letters indicate significant differences ($P \leq 0.05$) between the three sampling times for each treatment (PSM1, PSM2, SM, PS1 and PS2). Capital letters indicate significant differences ($P \leq 0.05$) between the treatments at a given sampling time. T_0 = 64 d; T_1 = 125 d and T_2 = 200 d. PSM1: C. *alternifolius* + electrode; PSM2: short leaf *C.malaccensis* + electrode; SM: electrode; PS1: *C. alternifolius*; PS2: short leaf *C. malaccensis*

than 10–20 cm, but lower concentrations than those at the 0–10 cm distance: 0–10 cm > 20–30 cm > 10–20 cm (Fig. 4c). Additionally, the total As concentrations at the 20–30 cm distance in the plant treatments (PSM1, PSM2, PS1 and PS2) were all higher than those in the SM treatment. This demonstrates that the electricity production of the electrode system inhibits the mobility of arsenic with the increasing distance from the anode due to processes occurring at the anode. In the distance of 20–30 cm, the plant also inhibited the mobility of arsenic. The arsenic concentrations were lower in the vicinity of the anode because the electricity production process of the anode inhibits the release/mobility of arsenic.

The total arsenic concentrations in the overlying water column for each treatment and sampling time are reported in Fig. 4d. The dissolved As concentrations for the PS1 and PS2 treatments were significantly higher than those for the PSM1, SM and PSM2 treatments. This is in agreement with the PS1 and PS2 treatments having significantly lower As concentrations in the sediments. With the increasing time, the labile As forms in the sediments decreased, resulting in a concomitant decrease in the As concentrations in the overlying water in the PSM1, SM and PSM2 treatments, possibly due to plant uptake. In addition, other As removal processes, such as microbial immobilization, methylation, release of volatile arsenic hydride into the atmosphere and the oxidation of As close to the anode of MFC, may further result in the loss of As from the MFC systems (Peng et al. 2009; Zhao et al. 2010; Lomax et al. 2012).

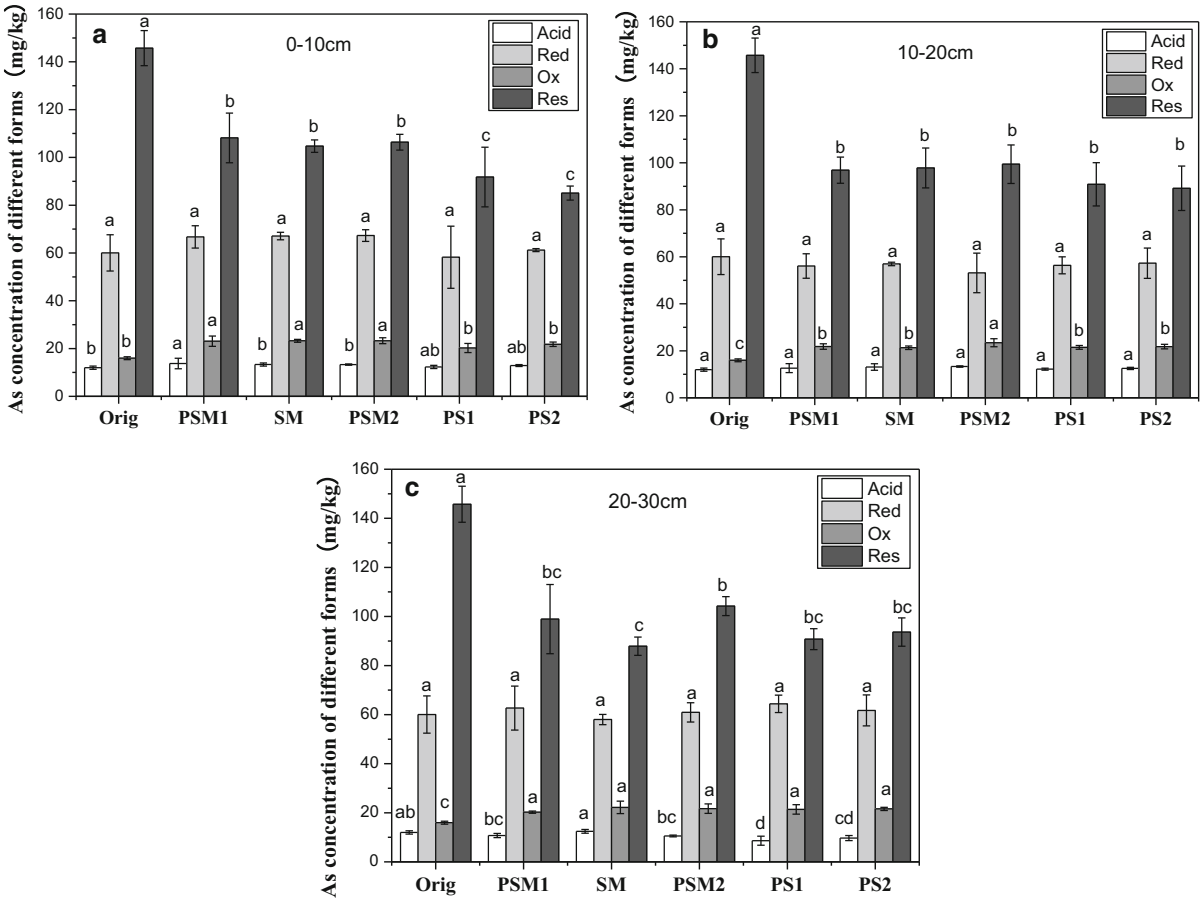

Fig. 5 Concentrations of different arsenic fractions in sediments (average of three replicates ± standard deviation). Lower-case letters indicate significant differences ($P \leq 0.05$) between the four arsenic fractions of each treatment. Orig: original sediment samples; PSM1: C. *alternifolius* + electrode; PSM2: short leaf *C. malaccensis* + electrode; SM: electrode; PS1: C. *alternifolius*; PS2: short leaf *C. malaccensis*. *Acid* acid-soluble arsenic, *Red* reducible arsenic, *Ox* oxidizable arsenic, *Res* residual arsenic

Based on the analysis above, the operating fuel cell systems resulted in a significant decrease in the arsenic sediment contents in all the treatments; the concentrations decreased more quickly in the PS1 and PS2 treatments than that in the PSM1, SM and PSM2 treatments. The electrode electricity production process was beneficial for immobilizing arsenic in the sediments, which attenuated the arsenic release into the overlying water column. The sediment arsenic concentrations were lower as the distance from the anode increased. Thus, the electricity production process at the anode inhibits the release/mobility of arsenic from the sediments and immobilizes As in the sediment resulting in a lower mobility in the water column and presumably a lower bioavailability.

After 200 days of fuel cell operation, the sediment samples (0–10, 10–20 and 20–30 cm from the anode) were analyzed to determine the changes in the solid-phase As fractions in the sediment. While the total As and residual arsenic contents in the sediments decreased, at 0–10 cm from the anode (Fig. 5a), the residual and oxidizable arsenic contents were significantly lower in the PS1 and PS2 treatments than that in the PSM1, SM and PSM2 treatments. This finding indicates that the electricity production process at the electrode stabilizes more of the residual and oxidizable As fractions. Previous studies have shown that the oxidation–reduction potential plays an important role in sediment adsorption and the release of heavy metals (Fitz and Wenzel 2002). The increase in the oxidation potential around the anode may result in arsenic

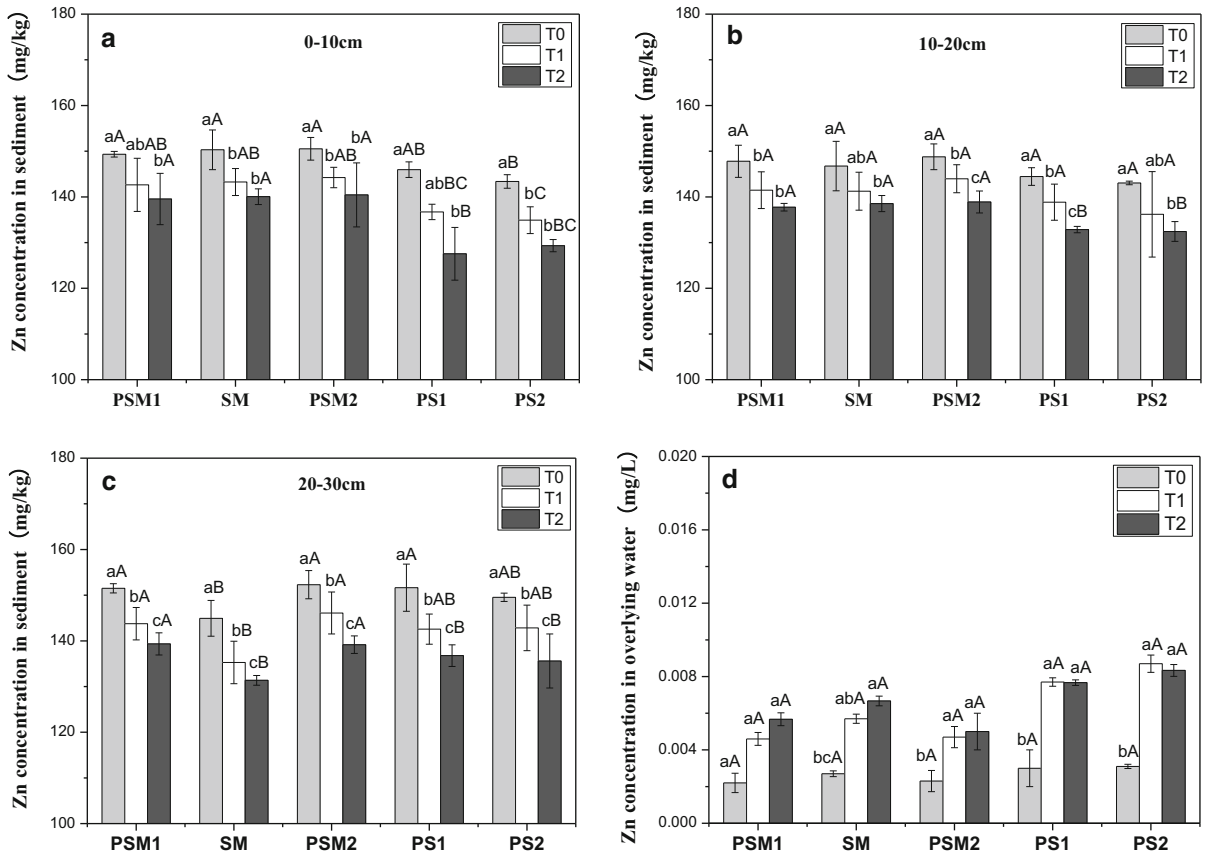

Fig. 6 Total Zn concentrations in the sediment and overlying water (average of three replicates ± standard deviation). Lower-case letters indicate significant differences ($P \leq 0.05$) between the three sampling times of each treatment (PSM1, PSM2, SM, PS1 and PS2). Capital letters indicate significant differences ($P \leq 0.05$) between the treatments at the same sampling time. T_0 = 64; T_1 = 125 and T_2 = 200 days. PSM1: C. *alternifolius* + electrode; PSM2: short leaf *C.malaccensis* + electrode; SM: electrode; PS1: *C. alternifolius*; PS2: short leaf *C.malaccensis*

oxidation around the electrode leading to higher concentrations of the oxidizable arsenic fraction.

There were few significant differences among the five treatments in the As fractions at distances of 10–20 and 20–30 cm from the anode (Fig. 5b, c). Thus, as the distance from the anode increased, the influence of the electrode was on the transformation of various arsenic forms in the sediment decreased. At a distance of 20–30 cm, i.e., the sediments closer to the plants, the acid-soluble As fraction concentrations followed the order: SM > PSM1 = PSM2 > PS1 = PS2. Possible explanations for this result include plant absorption of acid-soluble arsenic and oxidation of trivalent arsenite into pentavalent arsenate by microbial communities in the plant rhizosphere (Xiong et al. 2010; Lee et al. 2005).

In general, based on the operationally defined sequential extraction method, the bioelectricity process associated with the anode decreased the residual arsenic fraction and increased the oxidizable As fraction 0–10 cm from the anode. In the systems with plants, at a distance of 20–30 cm, i.e., the sediments closer to the plants, there was a small decrease in the acid-soluble arsenic fraction, possibly due to the uptake of this As fraction by plants.

Influence of the P-SMFC electricity production on the zinc content in sediments

Zinc concentrations in the sediments for each treatment and sampling time are reported in Fig. 6. Sediment zinc concentrations for the 0–10 and 10–20 cm sampling points of all the treatments

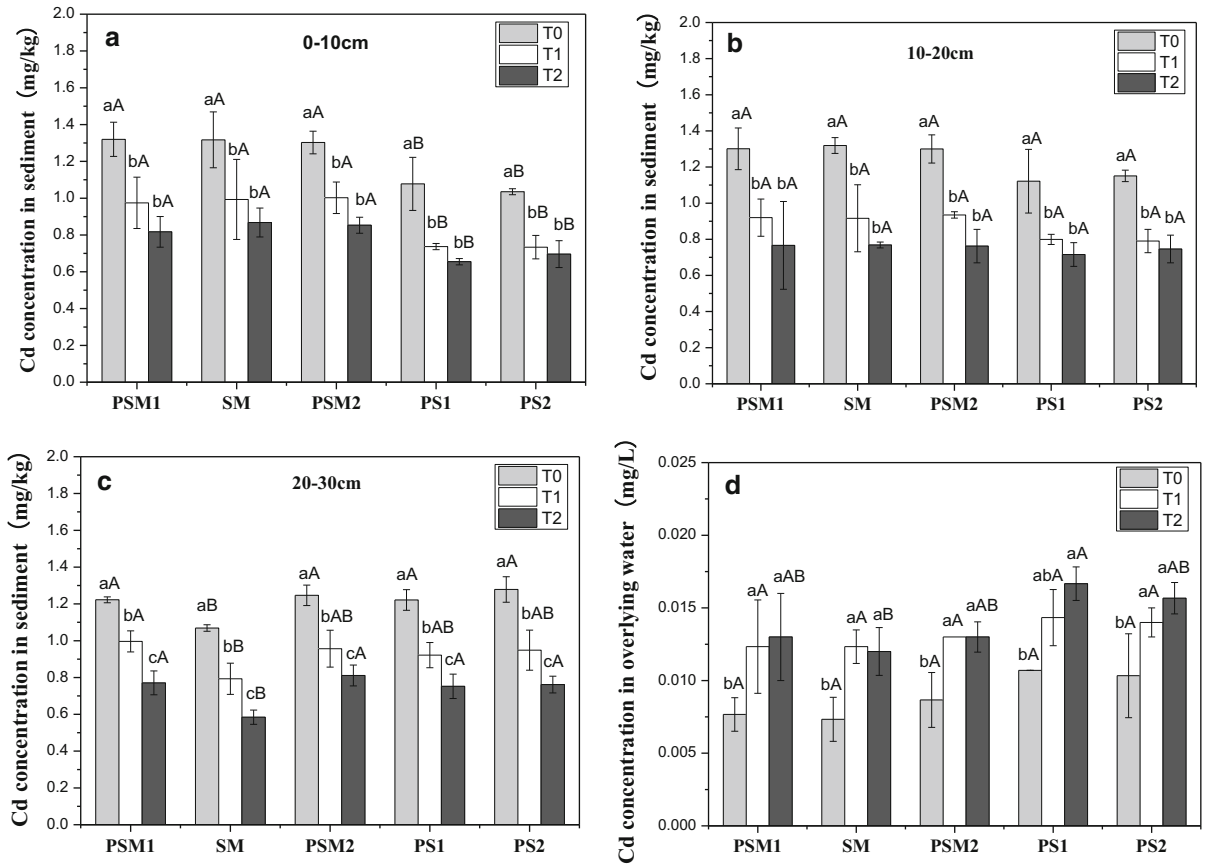

Fig. 7 Total Cd concentrations in the sediment and overlying water (average of three replicates ± standard deviation). Lower-case letters indicate significant differences ($P \leq 0.05$) between the three sampling times for each treatment (PSM1, PSM2, SM, PS1 and PS2). Capital letters indicate significant differences ($P \leq 0.05$) between the treatments at the same sampling time. $T_0 = 64$; $T_1 = 125$ and $T_2 = 200$ days. PSM1: C. *alternifolius* + electrode; PSM2: short leaf *C. malaccensis* + electrode; SM: electrode; PS1: *C. alternifolius*; PS2: short leaf *C. malaccensis*

showed similar patterns over time with a significant decrease after 125–200 days (Fig. 6a, b). By 200 days, the Zn levels in the PSM1, SM and PSM2 treatments at the 0–10 and 10–20 cm sampling points were significantly higher than those in the PS1 and PS2 treatments. This indicates that the electrode electricity production process immobilized the zinc in the sediment near the electrode. The reasons for this phenomenon may be that under anaerobic conditions, the anode electricity production uses sulfate and nitrate as the oxidant, which led to the formation of sulfide precipitation and contributed to the stabilization of heavy metals (Rabaey et al. 2006).

At the 20–30 cm sampling point, the differences in the zinc contents in the sediments among the treatments were not significant except for SM (Fig. 6c). The relationship between the dissolved zinc concentrations in the overlying water and the fuel cell operating time is shown in Fig. 6d. The dissolved Zn concentrations increased with time and were higher in the systems without plants but not significantly higher. Based on these analyses, the electrode electricity production process contributed to the stability of the zinc in the sediment, and as the distance from the anode increased, the zinc immobilization effect in the sediments decreased.

Influence of the P-SMFC electricity production on cadmium content in sediments

The total Cd content at the 0–10 cm distance was significantly higher in the fuel cell treatments (PSM1, SM and PSM2) than in the non-fuel cell treatments (PS1 and PS2) at all three sampling times (Fig. 7a).

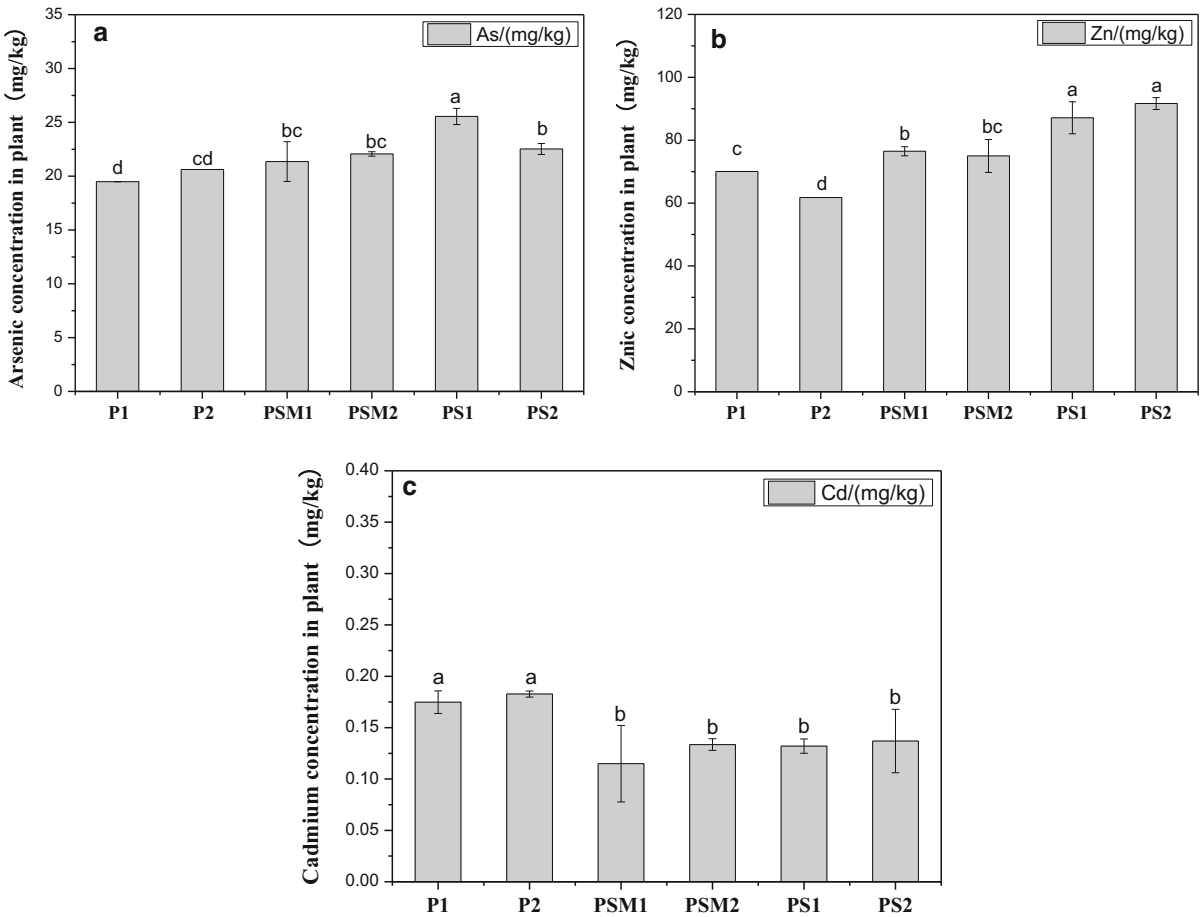

Fig. 8 Concentrations of As, Zn and Cd in plant tissues from the different treatments (average of three replicates ± standard deviation). Lower-case letters indicate significant differences ($P \leq 0.05$) between treatments. P1: initial metal concentration in *C. alternifolius*; P2: initial metal concentration in short leaf *C. malaccensis*; PSM1: *C. alternifolius* + electrode; PSM2: short leaf *C. malaccensis* + electrode; PS1: *C. alternifolius*; PS2: short leaf *C. malaccensis*

This demonstrates that the electrode electricity production process attenuated the loss of Cd from the sediments near the electrode. There were no significant differences between the treatments at the distances of 10–20 cm and 20–30 cm in the sediments (Fig. 7b, c), which indicated that the effects on the electrode processes were limited to the soil mass closest to the electrode, i.e., similar to Zn.

The dissolved Cd concentrations in the overlying water followed a pattern similar to that of the dissolved Zn (Fig. 7d). The dissolved Cd concentrations slowly increased with the processing time, and after 200 days, the SM treatment was generally lower than the plant-based treatments (PS1, PS2, PSM1 and PSM2).

Based on these analyses, the effects of the electrode electricity production are evident on the immobilization of Cd in the sediment in the vicinity of the electrode and decrease the release of Cd from the sediment into the overlying water.

Influence of the P-SMFC electricity production on the uptake of arsenic and heavy metals by plants

The As, Zn and Cd contents of plant tissues from the different treatments and pretreatment plants (P1 and P2) are reported in Fig. 8. The results show that the As and Zn concentrations in plant tissues increased (Fig. 8a, b), while the Cd concentrations decreased (Fig. 8c) during the experimental period. As and Zn accumulated in the plants during the experiment

because of the higher levels of As and Zn in the sediments, while Cd was present at low levels in the sediments. In addition, possibly, the plants were from an environment with higher levels of Cd concentrations, but this was not identified in this study.

All the plants in the treatments without electrodes (PS1 and PS2) accumulated ($P \leq 0.05$) higher levels of As and Zn than the P-SMFCs treatments (PSM1 and PSM2) by the end of the experiment (Fig. 8a, b), while the accumulation of Cd was not significant (Fig. 8c). The results show that the electrode electricity production process reduced the plant absorption of As and Zn from the sediments. In accordance with the discussion above, the electrode electricity production contributed to the stabilization and immobilization of As, Zn and Cd in the sediments, which decreased their bioavailability for wetland plants and release into the overlying water column.

Conclusions

The plants in the P-SMFC systems improved the bioelectricity production and efficiency. The average output voltages of the treatments were PSM1 (0.32 V) > PSM2 (0.28 V) > SM (0.24 V) ($P \leq 0.05$). The enhanced electricity production in the presence of plants is likely due to the higher levels of labile carbon associated with rhizosphere processes (e.g., plant exudates). The electricity production process resulted in the stabilization and immobilization of As, Zn and Cd in the sediments. The process increased the arsenic residual and oxidizable fractions, which demonstrated the redox transformation that occurred near the electrode. The effects of the electrode electricity process on the transformation of heavy metals were evident in the sediments within 10 cm or less of the anode, while the effects were diminished at greater distances. In the overlying water column, the dissolved As, Zn and Cd concentrations were lower in the fuel cell treatments (PSM1 and PSM2) than in the non-fuel cell treatments (PS1 and PS2). Furthermore, the plant tissues generally accumulated lower levels of As and Zn contents in the fuel cell treatments (PSM1 and PSM2) than in the non-fuel cell treatments (PS1 and PS2). The bioelectricity production enhanced the heavy-metal retention in the sediments and decreased the bioavailability of heavy metals, which indicates the potential use of P-SMFCs for the remediation of heavy-metal pollution in sediments.

Acknowledgements This study was financially supported by the Guangdong Provincial Science and Technology Project "Cooperation by production, study and research" (No. 2017A090905043 & 2017B090907012) and the Ministry of Science and Technology of China for State Key Research and Development Project (2016YFC0400702). The authors would like to thank Wang Jian and Shen Weihang for their assistance with the sample collection and preparation.

References

Abourached, C., Catal, T., & Liu, H. (2014). Efficacy of single-chamber microbial fuel cells for removal of cadmium and zinc with simultaneous electricity production. *Water Research, 51,* 228–233.

Audry, S., Schafer, J., Blanc, G., et al. (2004). Fifty-year sedimentary record of heavy metal pollution (Cd, Zn, Cu, Pb) in the Lot River reservoirs (France). *Environmental Pollution, 132*(3), 413–426.

Baig, J. A., Kazi, T. G., Arain, M. B., et al. (2009). Arsenic fractionation in sediments of different origins using BCR sequential and single extraction methods. *Journal of Hazardous Materials, 167*(1), 745–751.

Dalman, Ö., Demirak, A., & Balcl, A. (2006). Determination of heavy metals (Cd, Pb) and trace elements (Cu, Zn) in sediments and fish of the Southeastern Aegean Sea (Turkey) by atomic absorption spectrometry. *Food Chemistry, 95*(1), 157–162.

Das, H. K., Mitra, A. K., Sengupta, P. K., et al. (2004). Arsenic concentrations in rice, vegetables, and fish in Bangladesh: A preliminary study. *Environment International, 30*(3), 383–387.

Deng, D., & Dong, Y. (2016). Research on pollution and potential ecological risk of heavy metals in river sediment of typical areas in Jiangsu Province. *Environmental Science and Management, 4,* 042.

Duan, L. Q., Song, J. M., Yuan, H. M., et al. (2016). Distribution, partitioning and sources of dissolved and particulate nitrogen and phosphorus in the north Yellow Sea. *Estuarine, Coastal and Shelf Science, 181,* 182–195.

Fitz, W. J., & Wenzel, W. W. (2002). Arsenic transformations in the soil—rhizosphere—plant system: Fundamentals and potential application to phytoremediation. *Journal of Biotechnology, 99*(3), 259–278.

Heijne, A. T., Liu, F., van der Weijden, R., et al. (2010). Copper recovery combined with electricity production in a microbial fuel cell. *Environmental Science and Technology, 44*(11), 4376–4381.

Huang, L., Pu, X., Pan, J. F., et al. (2013). Heavy metal pollution status in surface sediments of Swan Lake lagoon and Rongcheng Bay in the northern Yellow Sea. *Chemosphere, 93*(9), 1957–1964.

Hung, C. V., Cam, B. D., Mai, P. T. N., et al. (2015). Heavy metals and polycyclic aromatic hydrocarbons in municipal sewage sludge from a river in highly urbanized

metropolitan area in Hanoi, Vietnam: Levels, accumulation pattern and assessment of land application. *Environmental Geochemistry and Health, 37*(1), 46–133.

Islam, M. S., Ahmed, M. K., Raknuzzaman, M., et al. (2015). Heavy metal pollution in surface water and sediment: A preliminary assessment of an urban river in a developing country. *Ecological Indicators, 48,* 282–291.

Kadhum, S. A., Ishak, M. Y., Zulkifli, S. Z., et al. (2015). Evaluation of the status and distributions of heavy metal pollution in surface sediments of the Langat River Basin in Selangor Malaysia. *Marine Pollution Bulletin, 101*(1), 391–396.

Lee, J. U., Lee, S. W., Kim, K. W., et al. (2005). The effects of different carbon sources on microbial mediation of arsenic in arsenic-contaminated sediment. *Environmental Geochemistry and Health, 27*(2), 159–168.

Lefebvre, O., Tan, Z., Shen, Y., et al. (2013). Optimization of a microbial fuel cell for wastewater treatment using recycled scrap metals as a cost-effective cathode material. *Bioresource Technology, 127,* 158–164.

Logan, B. E., Hamelers, B., Rozendal, R., et al. (2006). Microbial fuel cells: Methodology and technology. *Environmental Science and Technology, 40*(17), 5181–5192.

Lomax, C., Liu, W.-J., Wu, L., et al. (2012). Methylated arsenic species in plants originate from soil microorganisms. *New Phytologist, 193*(3), 665–672.

Nejad, Z. D., Jung, M. C., & Kim, K. H. (2018). Remediation of soils contaminated with heavy metals with an emphasis on immobilization technology. *Environmental Geochemistry and Health, 40,* 927–953.

Noe, G. B., Hupp, C. R., Bernhardt, C. E., et al. (2016). Contemporary deposition and long-term accumulation of sediment and nutrients by tidal freshwater forested wetlands impacted by sea level rise. *Estuaries and Coasts, 39,* 1–14.

Peng, J. F., Song, Y. H., Yuan, P., et al. (2009). The remediation of heavy metals contaminated sediment. *Journal of Hazardous Materials, 161*(2), 633–640.

Rabaey, K., Van de Sompel, K., Maignien, L., et al. (2006). Microbial fuel cells for sulfide removal. *Environmental Science and Technology, 40*(17), 5218–5224.

Sarria-Villa, R., Ocampoduque, W., Paez, M., et al. (2016). Presence of PAHs in water and sediments of the Colombian Cauca River during heavy rain episodes, and implications for risk assessment. *Science of the Total Environment, 540,* 455–465.

Schamphelaire, L. D., Van den Bossche, L., Dang, H. S., et al. (2008). Microbial fuel cells generating electricity from rhizodeposits of rice plants. *Environmental Science and Technology, 42*(8), 3053–3058.

Simmons, R. W., Pongsakul, P., Saiyasitpanich, D., et al. (2005). Elevated levels of cadmium and zinc in paddy soils and elevated levels of cadmium in rice grain downstream of a zinc mineralized area in Thailand: Implications for public health. *Environmental Geochemistry and Health, 27*(5), 501–511.

Stortelder, P. B. (1995). The management of contaminated sediment, an overview. *European Water Pollution Control, 5*(5), 8–15.

Tandukar, M., Huber, S. J., Onodera, T., Pavlostathis, S. G., et al. (2009). Biological chromium (VI) reduction in the cathode of a microbial fuel cell. *Environmental Science and Technology, 43*(21), 8159–8165.

Volesky, B., & Holan, Z. R. (1995). Biosorption of heavy metals. *Biotechnology Progress, 11*(3), 235–250.

Wang, G., Huang, L., & Zhang, Y. (2008). Cathodic reduction of hexavalent chromium [Cr(VI)] coupled with electricity generation in microbial fuel cells. *Biotechnology Letters, 30*(11), 1959–1966.

Wang, H., Song, H. L., Yu, R., et al. (2016). New process for copper migration by bioelectricity generation in soil microbial fuel cells. *Environmental Science and Pollution Research, 23*(13), 13147.

Xiong, J., Wu, L., Tu, S., et al. (2010). Microbial communities and functional genes associated with soil arsenic contamination and the rhizosphere of the arsenic-hyperaccumulating plant Pteris vittata L. *Applied and Environmental Microbiology, 76*(21), 7277–7284.

Yin, A., Yang, Z., Ebbs, S., et al. (2016). Effects of phosphorus on chemical forms of Cd in plants of four spinach (Spinacia oleracea L.) cultivars differing in Cd accumulation. *Environmental Science and Pollution Research, 23*(6), 5753–5762.

Zhang, W., Liu, X., Cheng, H., et al. (2012). Heavy metal pollution in sediments of a typical mariculture zone in South China. *Marine Pollution Bulletin, 64*(4), 712–720.

Zhao, F., McGrath, S. P., & Meharg, A. A. (2010). Arsenic as a food chain contaminant: Mechanisms of plant uptake and metabolism and mitigation strategies. *Annual Review of Plant Biology, 61,* 535–559.

Zhu, N., Chen, X., Zhang, T., et al. (2011). Improved performance of membrane free single-chamber air-cathode microbial fuel cells with nitric acid and ethylenediamine surface modified activated carbon fiber felt anodes. *Bioresource Technology, 102*(1), 422–426.